C. R. Chimie 17 (2014) 1102–1108

Contents lists available at ScienceDirect

Comptes Rendus Chimie

www.sciencedirect.com

Full paper/Mémoire

Blue-light-emitting and hole-transporting molecular materials based on amorphous triphenylamine-functionalized twisted binaphthyl

Xiao Fan, Zhongping Li, Dandan Yao, Yuwei Zhang, He Li, Xiaoming Liu *, Yue Wang, Ying Mu *

State Key Laboratory of Supramolecular Structure and Materials, College of Chemistry, Jilin University, 2699 Qianjin Street, Changchun 130012, PR China

ARTICLE INFO

Article history:
Received 11 September 2013
Accepted after revision 27 January 2014
Available online 18 September 2014

Keywords:
Blue organic light-emitting diodes
Hole-transporting
Amorphous materials
Triphenylamine
Binaphthyl

ABSTRACT

Two stable blue-light-emitting molecular materials containing twisted binaphthyl and peripheral triphenylamine groups were synthesized by Suzuki and Heck cross-coupling reactions. Both compounds exhibit excellent thermal and morphologic stabilities, high glass transition temperatures and good fluorescence quantum yield in films. They serve as both hole-transporting and blue emission materials in organic light-emitting diodes with good external quantum efficiencies.

1. Introduction

Conjugated organic molecules have attracted much attention due to their potential applications as optoelectronic and photonic materials in a number of fields, such as organic light-emitting diodes (OLEDs) [1], organic solar cells [2] and two-photon excited emitters [3]. Small π-conjugated organic molecules provide remarkable advantages, such as readily synthetic accessibility, well-defined molecular structures, facile purification by standard techniques, and specific structure–property correlations [4]. However, most of π-conjugated organic molecules have a strong tendency of aggregation in the solid state due to intermolecular interactions, which results easily in morphological changes, excimer formation, red-shifted emission and as well as low emission efficiency [5]. To overcome these disadvantages, several strategies, such as spiro [6], dendritic substituent protection [7], aggregation-induced emission [8] and J-aggregation formation [9] have been adopted for the design and construction of novel π-conjugated organic molecules with high quantum efficiency and good stabilities. In particular, functionalized bimesityls [10] and biphenyls [11] in which the chromophores are connected through the rotatable phenyl–phenyl or mesityl–mesityl bond have been developed. It was reported that the twisted configuration of these molecules suppresses intermolecular interactions, and thus enhances their photoluminescence (PL) and EL performance in the solid state.

It is well known that the chiral 1,1′-binaphthyl molecule possesses an inherent large dihedral angle, which can efficiently regulate its aggregation state with the binaphthyl. Pu et al. have reported the use of binaphthyl as a building block for the construction of π-conjugated polymers [12]. It was found that the incorporation of the twisted non-planar binaphthyl moiety into the conjugated polymer backbone could suppress the packing of the polymer chains in the aggregated state, which improved the fluorescent quantum efficiency. Up to

* Corresponding authors.
E-mail addresses: xm_liu@jlu.edu.cn (X. Liu), ymu@jlu.edu.cn (Y. Mu).

1631-0748/$ – see front matter
http://dx.doi.org/10.1016/j.crci.2014.01.022

now, however, small organic molecules based on binaphthyl were less reported and showed relatively low efficiency and luminescence [13]. From a synthetic point of view, the use of binaphthyl with an inherent twist as a building block for the construction of the organic molecules with high efficiency is also a simple and effective approach. We have now synthesized two simple organic molecules containing twisted binaphthyl and triphenylamine groups, and both provide several key features. First, the twisted geometry introduced by the binaphthyl hinders packing of molecules, leading to amorphous glass state, which is important for application as materials in OLEDs. Second, the introduction of the triphenylamine groups results in the fact that the compounds possess excellent hole-transport and injection properties. Third, the rigid connection makes that compounds have high glass transition (T_g) and decomposition temperatures. Here, we report the synthesis and characterization of the two compounds containing binaphthyl and triphenylamine groups, their photophysical and electrochemical properties in solution, as well as their EL performance in OLEDs as either the emitter or the hole-transporting material.

2. Experimental

2.1. Materials and methods

Manipulations of air- and moisture-sensitive materials were carried out under high-purity nitrogen atmosphere using standard Schlenk line or glove-box techniques. Tetrahydrofuran (THF) was dried under refluxing over sodium/benzophenone and distilled under nitrogen prior to use. *N*,*N*-Dimethylformamide (DMF) was dried by distilling over calcium hydride before use. BuLi, $Pd(OA_C)_2$, $Pd(PPh_3)_4$, 1,1′-binaphthalene-2,2′-diol (BINOL), Tri-(8-hydroxyquinolino)aluminum (Alq_3), 4,4-bis[*N*-(1-naphthyl)-*N*-phenylamino]biphenyl (NPB) and 1,3,5-tris(2-*N*-phenylbenzimidazolyl)benzene (TPBI) were purchased from Aldrich or Acros and used as received. NMR spectra were measured on either a Bruker AVANCE-500 NMR spectrometer or a Varian Mercury-300 NMR spectrometer. The elemental analysis was performed with a PerkinElmer 2400 microanalyzer. UV–vis absorption spectra were recorded on a Shimadzu UV-3600 spectrophotometer. Fluorescence measurements were carried out on a Shimadzu RF-5301PC spectrophotometer. Photoluminescent quantum yields for compounds **4** and **5** in ethyl acetate were measured at room temperature with an excitation wavelength of 360 nm, referenced to quinine sulfate in sulfuric acid aqueous solution ($\Phi = 0.546$) [14]. The solid state fluorescence quantum yields for both compounds were measured from freshly prepared films with Alq_3 as the standard. DSC measurements were performed on a NETZSCH DSC204 instrument. TGA experiments were carried out on a TA Q500 thermogravimeter. P-XRD analysis was performed on a Rigaku D/Max-2550 diffractometer using Cu Kα radiation, operating at 50 kV and 200 mA, and the data were collected in the 2θ range from 0 to 40° with a scanning rate of 1 °C/min. Cyclic voltammetry was performed on a CHI 660C instrument with a scan rate of 100 mV/s. A three-electrode configuration was used for the measurement: a platinum electrode as the working electrode, a platinum wire as the counter electrode, and an Ag/Ag^+ electrode as the reference electrode.

2.2. Synthesis

2.2.1. 6,6′-Bis[4′′-(diphenylamino)phenyl]-2,2′-dimethoxy-1,1′-binaphthyl (4)

A mixture of **1** (0.501 g, 1.06 mmol), **2** (0.650 g, 2.23 mmol) and $Pd(PPh_3)_4$ (40 mg) in THF (30 mL), and a K_2CO_3 aqueous solution (2 M, 10 mL) were heated to reflux under N_2 overnight. The reaction mixture was extracted with dichloromethane (3 × 50 mL) and water (100 mL), and the organic phase was separated, dried over anhydrous $MgSO_4$, filtered and evaporated to give the crude product. Further purification by column chromatography gave the pure product **4** as a white powder (0.461 g, 0.576 mmol, 54%). ^{1}H NMR ($CDCl_3$, 500 MHz, 298 K): δ 8.02 (d, 4H, Ar*H*), 7.55 (d, 4H, Ar*H*), 7.48 (d, 4H, Ar*H*), 7.29–7.12 (m, 22H, Ar*H*), 7.03 (t, 4H, Ar*H*), 3.80 (s, 6H, C*H*$_3$) ppm. ^{13}C ($CDCl_3$, 75 MHz, 298 K): δ 56.8, 114.5, 119.7, 122.9, 123.7, 124.1, 124.4, 125.7, 127.3, 127.6, 129.2, 129.5, 131.9, 132.9, 133.5, 147.2, 147.6, 155.2 ppm. Ms *m/z*: 800.3 $[M]^+$ (calcd: 800.34). Anal. calcd (%) for $C_{58}H_{44}N_2O_2$: C, 86.07; H, 5.54; N, 3.50. Found: C, 86.15; H, 5.60; N, 3.55.

2.2.2. 6,6′-bis[4′′-(diphenylamino)phenylvinyl]-2,2′-dimethoxy-1,1′-binaphthyl (5)

A mixture of **1** (0.501 g, 1.06 mmol), **3** (0.610 g, 2.23 mmol), K_2CO_3 (1.46 g, 10.6 mmol), ^{t}Bu$_4$NBr (0.32 g, 0.10 mmol) and $Pd(OA_C)_2$ (25 mg, 0.11 mmol) in dry DMF (5 mL) was heated at 110 °C under N_2 for 36 h. The reaction mixture was cooled to room temperature, quenched with water (100 mL) and extracted with CH_2Cl_2 (3 × 50 mL). The organic phase was dried over anhydrous $MgSO_4$, filtered and evaporated to give the crude product, which was further purified by column chromatography to give the pure product **5** as a white solid (0.375 g, 0.439 mmol, 41%). ^{1}H NMR ($CDCl_3$, 500 MHz, 298 K): δ 7.96 (d, 2H, Ar*H*), 7.86 (s, 2H, Ar*H*) 7.48–7.38 (m, 8H, Ar*H*), 7.28–7.23 (m, 4H, Ar*H*), 7.12–7.00 (m, 22H, Ar*H*), 6.70–6.90 (d, 4H, =C*H*), 3.78 (s, 6H, C*H*$_3$) ppm. ^{13}C ($CDCl_3$, 75 MHz, 298 K): δ 56.9, 114.7, 119.6, 122.8, 124.0, 124.4, 125.8, 127.8, 129.2, 129.5, 129.6, 133.0, 135.1, 135.7, 146.9, 147.7, 155.0 ppm. Ms *m/z*: 853.3 $[M]^+$ (calcd: 852.37). Anal. calcd (%) for $C_{62}H_{48}N_2O_2$: C, 87.29; H, 5.67; N, 3.28. Found: C, 87.35; H, 5.80; N, 3.11.

2.3. Device fabrication

Indium–tin oxide (ITO)-coated glass was used as the substrate, which was cleaned by sonication in a detergent solution, acetone, methanol, and deionized water before use. The devices were fabricated under a pressure of 5×10^{-6} Torr with the organic layers being deposited onto the substrate at a rate of 1–2 Å/s. Compound **4** or **5** was either used as an emitting layer material or a hole-transporting layer material, respectively. Alq_3 and TPBI were used as the electron-transporting layer materials, and NPB was used as the hole-transporting layer material. LiF and aluminum were evaporated as the cathode layers of

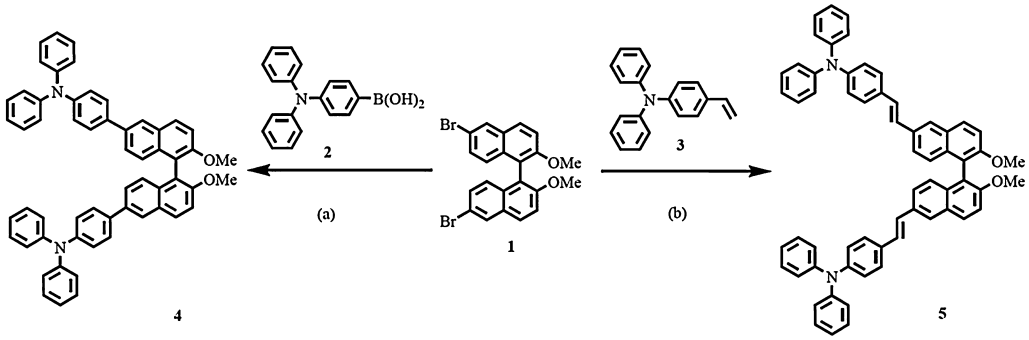

Scheme 1. Synthetic route for compounds **4** and **5**: (a) $Pd(PPh_3)_4$, K_2CO_3, THF, 90 °C; (b) $Pd(OAc)_2$, K_2CO_3, Bu_4NBr, DMF, 110 °C.

the device. The thicknesses of the organic materials and the cathode layers were controlled using a quartz crystal thickness monitor. Alq_3, NPB, TPBI, compounds **4** and **5** were further purified by vacuum sublimation before use.

3. Results and discussion

3.1. Synthesis, morphologic character, photophysical and electrochemical properties

Two target compounds **4** and **5** were prepared as shown in Scheme 1. The 1,1′-binaphthyl derivatives **1** and the triphenylamine derivatives **2** and **3** were synthesized according to related literature procedures [15]. Compound **4** was finally obtained as a white solid in 55% yield by Suzuki cross-coupling between **1** and **2** in the presence of $Pd(PPh_3)_4$ and K_2CO_3 in THF, while compound **5** was synthesized as yellowish powders in 42% yield by Heck cross-coupling between **1** and **3** in DMF using $Pd(OAc)_2$ as the catalyst. The structures of compounds **4** and **5** were confirmed by elemental analyses, NMR and MALDI-TOF MS spectroscopic techniques.

The morphologic character of compounds **4** and **5** was investigated by thermal analysis and powder X-ray diffraction measurements. Differential scanning calorimetric (DSC) and thermogravimetric analysis (TGA) measurements were performed under nitrogen atmosphere, and the results were shown in Fig. 1. The DSC curves show T_g at 117 °C for **4** and 139 °C for **5**, and the TGA profiles evidence their decomposition temperatures (with a 5% weight loss) at 401 and 432 °C, respectively. No phase change corresponding to melting or crystallization was observed in the DSC curves for both compounds upon heating from 30 to 300 °C. Upon cooling from the melts, both compounds have been transformed to the glassy state. The results reveal that the twisted binaphthyl moiety can efficiently hinder the crystallization process. It is well known that amorphous materials are necessary for fabricating high-quality OLEDs. To further validate morphologic properties in details, the powder X-ray diffraction analysis for compounds **4** and **5** was determined on quartz substrates (Fig. 2). As can be seen, two compounds show comparatively broad and random scattered peaks,

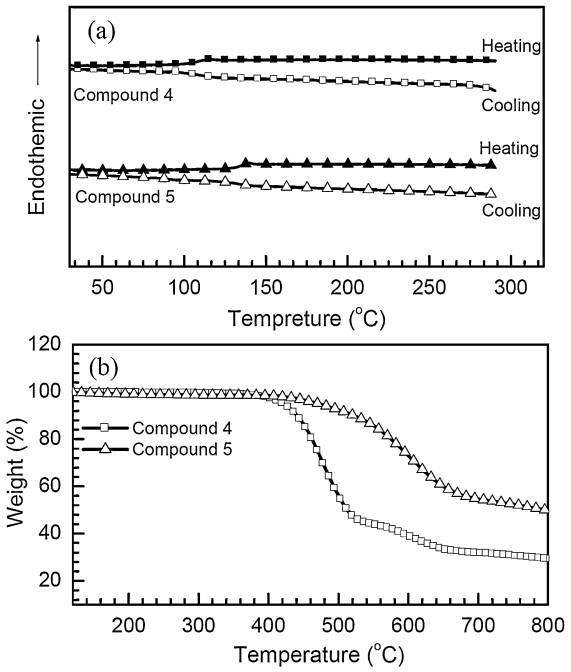

Fig. 1. DSC (a) and TGA (b) curves of **4** and **5** under nitrogen atmosphere at a heating rate of 10 °C/min.

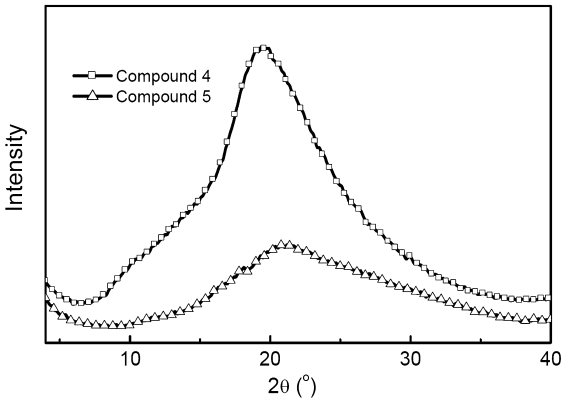

Fig. 2. Powder X-ray diffraction patterns of compounds **4** and **5** at room temperature.

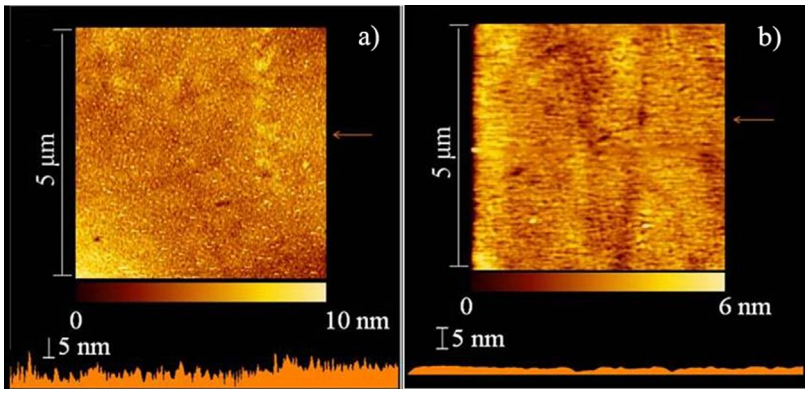

Fig. 3. (Color online.) AFM images of **4** (a) and **5** (b).

indicating the non-crystalline amorphous feature in the solid state. The film-forming ability of two compounds was also examined by vacuum-depositing them onto quartz glass to fabricate their films. Atomic force microscopy (AFM) was employed to explore the surface image of the films and revealed similar smooth and uniform topographies, free of pinholes, particle aggregation, or phase separation, with root-mean-square surface roughness values of about 0.60 nm (Fig. 3).

Fig. 4 shows the absorption and emission spectra of two compounds in ethyl acetate and in films, respectively. More details about their photophysical properties are listed in Table 1. In solution, compound **4** shows an absorption peak around 335 nm, while compound **5** evidences absorption at 375 nm, with a red shift of

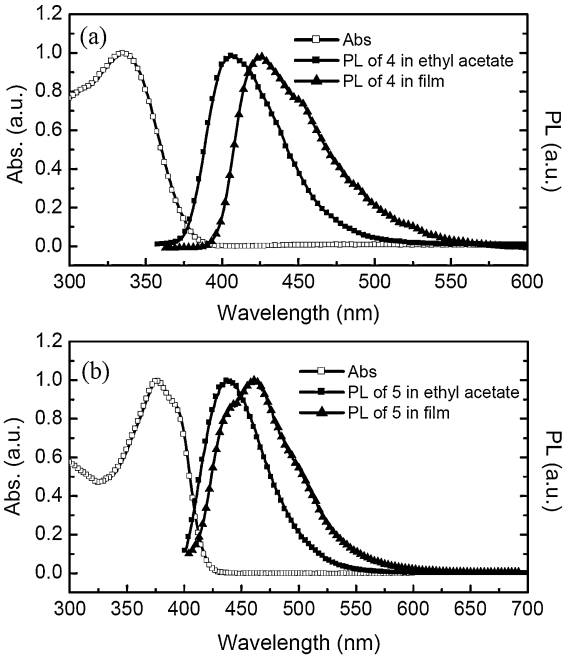

Fig. 4. Absorption and emission spectra of **4** and **5** in ethyl acetate (1×10^{-5} M) and films.

40 nm in comparison to that of **4** due to the incorporation of the C=C bridging group between the triphenylamine and binaphthyl chromophores. Upon irradiation with an excited light, both compounds exhibit very strong blue fluorescence in ethyl acetate solution, with emission peaks at 405 nm for **4** and 439 nm for **5**, respectively. In comparison to **4**, compound **5** possesses a longer π-conjugated structure and thus greater electron delocalization, which results in the red shift in both its absorption and emission spectra. In addition, high fluorescence quantum yields were obtained for both compounds **4** (71%) and **5** (80%) in ethyl acetate solution. In the different solutions, two compounds show obvious solvatochromism and their emission maxima shift to long wavelength with the increase in solvent polarity, as seen from the results in Fig. 5. For example, the emission maximum of the compound **5** appears at 414 nm in *n*-hexane, 447 nm in toluene, 462 nm in chloroform and 483 nm in CH_3CN, respectively. The insets in Fig. 5 show the photographs of compounds **4** and **5** in different solvents under UV irradiation at 365 nm. The strong solvent dependence of emission frequency demonstrates the presence of a highly polarized exited state, which is attributed to the charge transfer between the triphenylamine and binaphthyl units in both molecules [16]. The solid films of **4** and **5** were fabricated by spin-coating from their dichloromethane solutions. They display blue fluorescence with emission peaks at 423 and 461 nm, respectively. The emission maxima of **4** and **5** in the solid films show a red shift of about 20 nm compared to those in ethyl acetate solution, however, the spectra is still local in the blue-light region. The red shift phenomenon can be attributed to the π-stacking of the aromatic rings in molecules in the solid state. In addition, the two compounds exhibit good PL quantum yield (21% for **4** and 33% for **5**) in films, which is attributed to a reduction of the probability of intermolecular interactions and prevent close packing in the solid state.

The electrochemical properties of compounds **4** and **5** were investigated by cyclic voltammetry (CV) measurements and the results were listed in Table 1. The relevant cyclic voltammograms are given in Fig. 6. Two compounds show an irreversible reduction reaction with reduction

Table 1
Optical absorption, photoluminescence, quantum yield, electrochemical data and thermal properties of **4** and **5**.

Compound	λ_{abs} (nm)[a]	λ_{em} (nm)[b]	λ_{em} (nm)[c]	Φ film	E^{ox}_{onset} (V)[d]	HOMO (eV)[e]	LUMO (eV)[f]	T_g (°C)	T_d (°C)
4	335	393	423	0.21	+0.53	−5.24	−2.04	117	401
5	375	439	461	0.33	+0.52	−5.23	−2.31	139	432

[a] Maximum absorption wavelength, measured in ethyl acetate.
[b] Maximum emission wavelength, measured in ethyl acetate.
[c] Maximum emission wavelength, measured in the solid state.
[d] Estimated by CV using a glass carbon disk as working electrode, platinum wire as auxiliary electrode, Ag/Ag^+ as a reference electrode, $[^nBu_4N][PF_6]$ as supporting electrolyte in tetrahydrofuran.
[e] Calculated from the E^{ox}_{onset}.
[f] Estimated from the HOMO and the optical bandgap.

potentials at about 1.9 V, which can be assigned to the redox couple of the binaphthyl segment. In contrast, reversible oxidation reactions with potentials of −0.53 and −0.52 V were observed for compounds **4** and **5**, respectively, which could be ascribed to the oxidation of the triphenylamine unit of the compounds. The HOMO energy levels of the compounds, estimated from their first oxidation potential, are −5.32 eV for **4** and −5.33 eV for **5**, respectively. These data reveal that the introduction of the triphenylamine unit to the molecules lowers the barrier height of these complexes for hole injection, thereby, facilitating hole transfer.

3.2. Electroluminescent properties

Further, we studied the electroluminescence properties of **4** and **5** with strong blue emission, high fluorescence quantum yields, excellent thermal stability, and good hole-transporting ability (Fig. 7). They were used to fabricate two types of device to evaluate their EL performance. The relevant data of the optimized devices were summarized in Table 2. One type of devices has a double-layer structure with the configuration of [ITO/compound (25 nm)/Alq_3 (70 nm)/LiF (0.5 nm)/Al (200 nm)] in which **4** (device A1) and **5** (device A2) are used as the hole-transporting material, with Alq_3 as both the emitter and electron-transporting materials. It was found that the device have an electroluminescent peak at 524 nm, which is attributed to the emission of Alq_3, and without emission with longer wavelength from the exciplex species. The device A1 shows the maximum brightness of 16,070 cd/m^2 at 20.5 V and the maximum current efficiency of 3.99 cd/A at 18.5 V, which is close to the reported results obtained with similar compounds [13a]. The other type of device we fabricated are the typical three-layer devices with the configuration of [ITO/NPB (25 nm)/compound (1 nm)/TPBI (50 nm)/LiF (0.5 nm)/Al (200 nm)] (device B1 and B2), in which an additional NPB material is used as the hole-transporting layer to characterize the emitting nature of compounds **4** (device B1) and **5** (device B2). These devices were found to produce blue electroluminescence with peaks at 439 and 448 nm for B1 and B2, respectively. The emission maxima of both compounds in the EL spectra of the three-layer devices match well with their thin-film PL spectra,

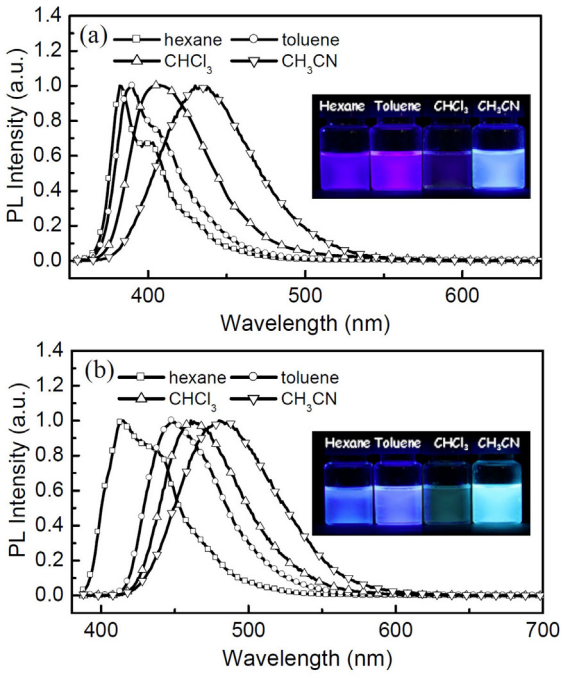

Fig. 5. (Color online.) Emission spectra of compounds **4** and **5** in different solvents ($M = 1 \times 10^{-5}$ mol/L).

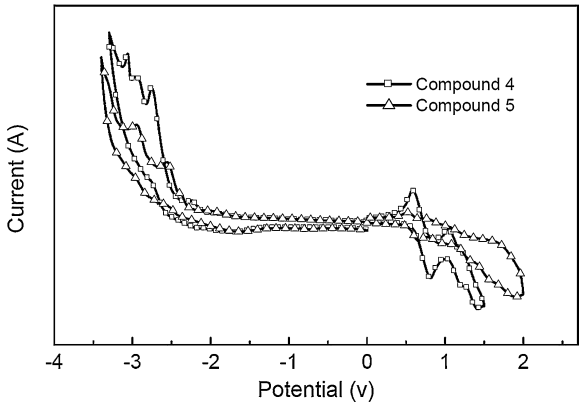

Fig. 6. Cyclic voltammograms of compounds **4** and **5**.

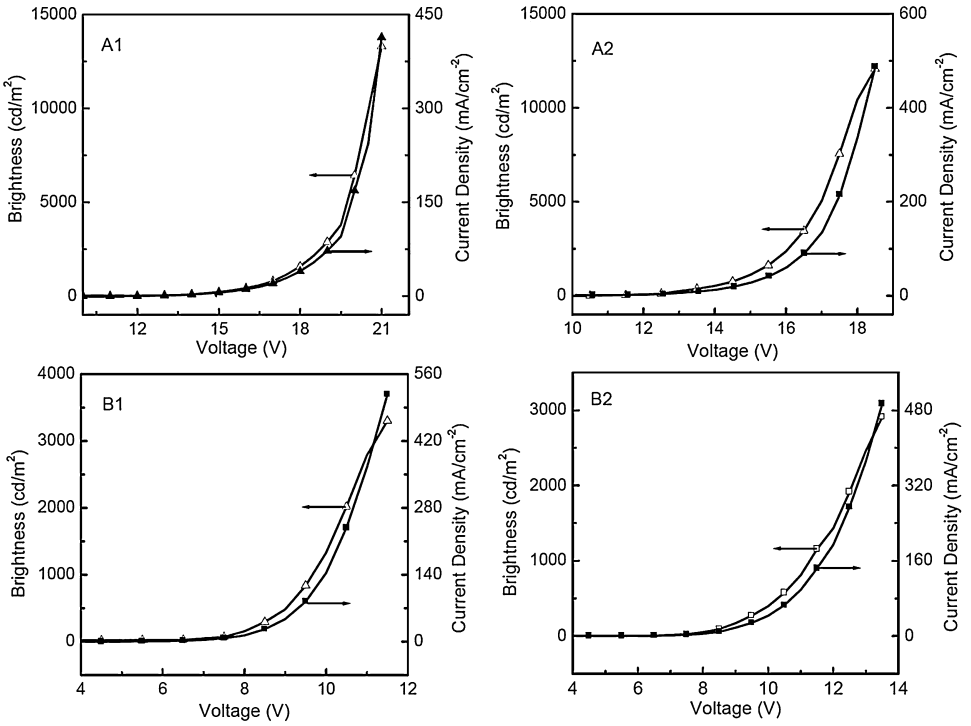

Fig. 7. Luminance-voltage-current (*L*–*V*–*J*) characteristics of devices.

indicating that EL originates from the intrinsic emissions of compounds **4** and **5**, respectively (Fig. 8). Device B1 with compound **5** as the emitter shows the maximum brightness of 3302 cd/m^2 at 11.5 V and the maximum current efficiency of 1.16 cd/A at 7.5 V. Similar results were obtained from device B2. These results are close to previously reported performances for OLEDs based on anthracene-containing binaphthol chromophores compounds (0.7–1.5 cd/A) [13b], dispiro-Xanthene-indenofluorene (1.0 cd/A) [17], fluorine-based compounds TCPC-6 (1.35 cd/A) [18]. However, they are lower than with the anthracene derivative with a tetraphenylethylene group (3.1 cd/A) [19], the pyrene-functionalized carbazole derivative (2.53 cd/A) [20] and device based on benzene-linked tetraphenylethene compounds (2.3–5.0 cd/A) [21]. Both A and B types of device have the advantages of low operating voltages and narrow EL luminance peaks. These results demonstrate that compounds **4** and **5** are potentially good hole-transporting and blue-emitter materials.

Table 2
Parameters of the EL devices based on compounds **4** and **5**.

Device	λ_{max} (nm)[a]	$V_{turn\text{-}on}$ (v)	B_{max} (cd/m^2)[b]	η_{max} (cd/A)[c]	CIE (*x*, *y*)
A1	524	7.4	16,070	3.99	0.34, 0.54
A2	524	8.5	12,640	4.19	0.32, 0.55
B1	439	4.7	3302	1.16	0.17, 0.13
B2	448	3.1	2909	1.01	0.18, 0.17

[a] Maximum EL emission wavelength.
[b] Maximum brightness.
[c] Maximum current efficiency.

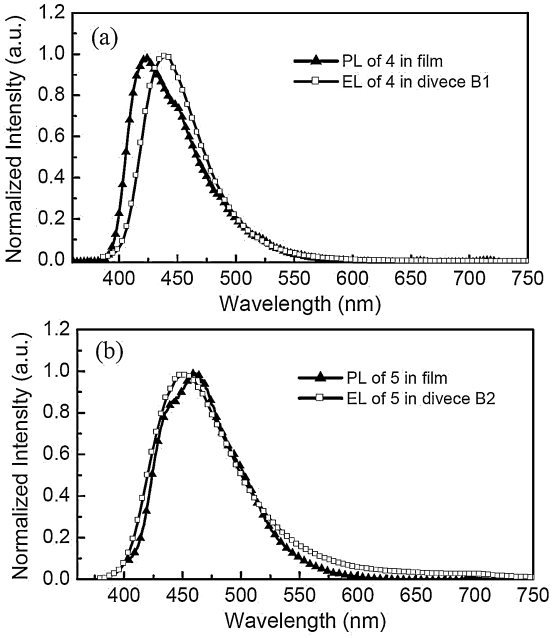

Fig. 8. PL spectra for films and EL spectra for device B of compound **4** (a) and **5** (b).

4. Conclusion

Two stable and amorphous light-emitting molecular materials containing twisted binaphthyl were synthesized by Suzuki and Heck cross-coupling reactions. They show excellent thermal and morphologic stabilities, high glass transition temperatures and good fluorescence quantum yield in films. Both compounds serve as both hole-transporting and blue emission materials in organic light-emitting diodes, with high external quantum efficiencies and simple structures.

Acknowledgements

This work was supported by the National Natural Science Foundation of China (Nos. 51203058, 21074043, and 51173061). X. Liu is also grateful for support from the Frontiers of Science and Interdisciplinary Innovation Project of Jilin University (No. 450060481015).

References

[1] (a) A.L. Kanibolotsky, I.F. Perepichkazbc, P.J. Skabara, Chem. Soc. Rev. 39 (2010) 2695;
(b) A. Chaskar, H.F. Chen, K.T. Wong, Adv. Mater. 23 (2011) 3876;
(c) H. Sasabe, J. Kido, Chem. Mater. 23 (2011) 621;
(d) S.L. Tao, Y.L. Jiang, S.L. Lai, M.K. Fung, Y.C. Zhou, X.H. Zhang, W.M. Zhao, C.S. Lee, Org. Electron 12 (2011) 358.
[2] J. Kwon, M.K. Kim, J.P. Hong, W. Lee, S. Noh, C. Lee, S. Lee, J.I. Hong, Org. Electron 11 (2010) 1288.
[3] S.L. Oliveira, D.S. Correa, L. Misoguti, C.J.L. Constantino, R.F. Aroca, S.C. Zilio, C.R. Mendonca, Adv. Mater. 17 (2005) 1890.
[4] H. Li, Z. Chi, B. Xu, X. Zhang, Z. Yang, X. Li, S. Liu, Y. Zhang, J. Xu, J. Mater. Chem. 20 (2010) 6103.
[5] (a) Y. Shirota, J. Mater. Chem. 15 (2005) 75;
(b) A.C. Grimsdale, Curr. Org. Chem. 14 (2010) 2196.
[6] (a) C. Poriel, J. Rault-Berthelot, D. Thirion, F. Barrière, L. Vignau, Chem. Eur. J. 17 (2011) 14031;
(b) C. Poriel, N. Cocherel, J. Rault-Berthelot, L. Vignau, O. Jeannin, Chem. Eur. J. 17 (2011) 12631;
(c) T.P.I. Saragi, T. Spehr, A. Siebert, T. Fuhrmann-Lieker, J. Salbeck, Chem. Rev. 107 (2007) 1011;
(d) Y.J. Cho, O.Y. Kim, J.Y. Lee, Org. Electron 13 (2012) 351.
[7] T. Qin, G. Zhou, H. Scheiber, R.E. Bauer, M. Baumgarten, C.E. Anson, E.J.W. List, K. Müllen, Angew. Chem. Int. Ed. 47 (2008) 8292.
[8] Z. Zhao, S. Chen, J.W.Y. Lam, Z. Wang, P. Lu, F. Mahtab, H.H.Y. Sung, I.D. Williams, Y. Ma, H.S. Kwokc, B.Z. Tang, J. Mater. Chem. 21 (2011) 7210.
[9] Z.Q. Xie, B. Yang, F. Li, G. Cheng, L.L. Liu, G.D. Yang, H. Xu, L. Ye, M. Hanif, S.Y. Liu, D.G. Ma, Y.G. Ma, J. Am. Chem. Soc. 127 (2005) 14152.
[10] (a) J.N. Moorthy, P. Venkatakrishnan, P. Natarajan, D.F. Huang, T.J. Chow, J. Am. Chem. Soc. 130 (2008) 17320;
(b) J.N. Moorthy, P. Venkatakrishnan, P. Natarajan, Z.H. Lin, T.J. Chow, J. Org. Chem. 75 (2010) 2599;
(c) J.N. Moorthy, P. Venkatakrishnan, P. Natarajan, D.F. Huang, T.J. Chow, Chem. Commun. (2008) 2146.
[11] (a) F. He, G. Cheng, H.Q. Zhang, Y. Zheng, Z.Q. Xie, B. Yang, Y.G. Ma, S.Y. Liu, J.C. Shen, Chem. Commun. (2003) 2206;
(b) F. He, H. Xia, S. Tang, Y. Duan, M. Zeng, L.L. Liu, M. Li, H.Q. Zhang, B. Yang, Y.G. Ma, S.Y. Liu, J.C. Shen, J. Mater. Chem. 14 (2004) 2735.
[12] (a) L. Pu, Macromal. Rapid Commun. 21 (2000) 795;
(b) L.X. Zheng, R.C. Urian, Y.Q. Liu, A.K.Y. Jen, L. Pu, Chem. Mater. 12 (2000) 13;
(c) J. Miyake, Y. Chujo, J. Polym. Sci. Part A: Polym. Chem. 46 (2008) 6035;
(d) Z.T. Liu, Y.M. He, Z.J. Wang, Y. Feng, Q.H. Fan, J. Polym. Sci. Part A: Polym. Chem. 46 (2008) 886.
[13] (a) Q. He, H. Lin, Y. Weng, B. Zhang, Z. Wang, G. Lei, L. Wang, Y. Qiu, F. Bai, Adv. Funct. Mater. 16 (2006) 1343;
(b) H. Benmansour, T. Shioya, Y. Sato, G.C. Bazan, Adv. Funct. Mater. 13 (2003) 883;
(c) Y. Zhou, Q.G. He, Y. Yang, H.Z. Zhong, C. He, G.Y. Sang, W. Liu, C.H. Yang, F.L. Bai, Y.F. Li, Adv. Funct. Mater. 18 (2008) 3299;
(d) Q.G. He, Z.Z. Chu, G.T. Lei, A.J. Qin, H.Z. Lin, F.L. Bai, J.G. Cheng, Y. Qiu, Chin. Chem. Lett. 19 (2008) 431.
[14] K. Ye, J. Wang, H. Sun, Y. Liu, Z. Mu, F. Li, S. Jiang, J. Zhang, Y. Wang, C.M. Che, J. Phys. Chem. B 109 (2004) 8008.
[15] (a) D.J. Cram, R.C. Helgeson, S.C. Peacock, L.J. Kaplan, L.A. Domeier, P. Moreau, K. Koga, J.M. Mayer, Y. Chao, J. Org. Chem. 43 (1978) 1930;
(b) V. Promarak, M. Ichikawa, D. Meunmart, T. Sudyoadsuk, S. Saengsuwan, T. Keawin, Tetrahedron Lett. 47 (2006) 8949;
(c) H.J. Xia, J.T. He, B. Xu, S.P. Wen, Y.W. Li, W.J. Tian, Tetrahedron 64 (2008) 5736.
[16] (a) W.L. Jia, M.J. Moran, Y.Y. Yuan, Z.H. Lu, S.N. Wang, J. Mater. Chem. 15 (2005) 3326;
(b) Y. Kubo, M. Yamamoto, M. Ikeda, M. Takeuchi, S. Shinkai, S. Yamaguchi, K. Tamao, Angew. Chem., Int. Ed. 42 (2003) 2036.
[17] N. Cocherel, C. Poriel, L. Vignau, J.-F. Bergamini, J.-R. Berthelot, Org. Lett. 12 (2010) 452.
[18] S. Tang, M.R. Liu, P. Lu, H. Xia, M. Li, Z.Q. Xie, F.Z. Shen, C. Gu, H.P. Wang, B. Yang, Y.G. Ma, Adv. Funct. Mater. 17 (2007) 2869.
[19] P.I. Shih, C.Y. Chuang, C.H. Chien, E.W.G. Diau, C.F. Shu, Adv. Funct. Mater. 17 (2007) 3141.
[20] P. Kotchapradist, N. Prachumrak, R. Tarsang, S. Jungsuttiwong, T. Keawin, T. Sudyoadsuk, V. Promarak, J. Mater. Chem. 1 (2013) 4916.
[21] J. Huang, N. Sun, J. Yang, R.L. Tang, Q.Q. Li, D.G. Ma, J.G. Qin, Z. Li, J. Mater. Chem. 22 (2012) 12001.